E-ISSN: 2582-6336

International Journal of Agriculture and Allied Sciences, 5(1); 4-10: 2020

PERFORMANCE ANALYSIS OF GRID CONNECTED RENEWABLE ENERGY SYSTEM WITH MULTILEVEL NPC INVERTER

ANCHAL YADAV

Research Scholar, Electrical Engineering Department
SHUATS Allahabad 211007, Sweet.anchal81@gmai.com

ABSTRACT

In recent years, multilevel inverters have gained popularity with medium and high power ratings. Photovoltaic solar panels, wind turbines, fuel cells and similar renewable energy sources can be interfaced to a multilevel converter system. The power of wind, one of the most abundant renewable sources of energy in nature, can be harnessed by a wind energy conversion system (WECS) composed of a wind turbine, an electric generator, a power electronic converter and the corresponding control system. The most advanced generator type is perhaps the permanent magnet synchronous generator (PMSG). The wind energy is connected to ac grid connected load. The loads in a grid may be unbalanced and non-linear in nature. Hence, injection of harmonic and unbalanced currents into the grid should be avoided since these harmonic currents and negative sequence currents (due to unbalance) will cause an unnecessary increase in the line currents. The solution to these problems is to use effective controllers with multilevel inverters. A multilevel inverter is used to step up the voltage and to reduce the THD. In this case, a nine-level and an eleven-level inverter are used and the voltage increases and THD decrements from 12.87% to 4.38%. Active and reactive power is controlled by DC stabilization and the reactive power is close to unity. An LC filter is used to eradicate the harmonics present in the system. For the performance evaluation of the proposed approach, a model of the AC grid, non-linear load, multilevel inverter and renewable energy resources (e.g., wind power generation) was developed in a MATLAB / SIMULINK environment.

KEYWORDS: Wind Energy, PMSM, Total Harmonic Distortion, Multilevel Inverter.

INTRODUCTION

The energy demand in today's world is continually increasing. This has entailed the investment of huge amounts of resources, both economical and human; to develop new technologies capable of production, transmission and conversion of the requisite electric power. In addition, the dependence on fossil fuels and the progressive increase of its cost has led to the appearance of new, economic and cleaner energy resources. In recent past, renewable energy resources have been the focus for researchers and various types of power converters have been designed in order to integrate these types of supplies into the distribution grid. Besides generation, a key requirement of electric power transmission is high-power electronic systems to assure conversion and quality energy output.

Numerous industry applications, such as textile and paper industry, steel mills, electric and hybrid electric vehicles, ship propulsion, railway traction, 'more-electric' aircraft, etc., for example, require utilization of variable speed electric drives. As far as the variable speed operation of electric drives is concerned, this is nowadays invariably achieved by supplying power to the machine, regardless of the type, from a power electronic converter.

Thus, power electronic converters have the responsibility to carry out these tasks with high efficiency. At each of these stages, the rapid development of power electronics has led to the implementation of new power conversion topologies and semiconductor technologies.

A continuous race to develop high-voltage and high-current power semiconductors to drive high-power systems still goes on. In this way, the last-generation devices are suitable to support high voltages and currents (around 6.5 kV and 2.5 kA). However, currently there is a tough competition between the use of classic power conversion topologies which use high-voltage semiconductors and new conversion topologies which use medium-voltage devices. Multilevel converters built using mature, medium-power semiconductors are competing with classic power converters which use high-power semiconductors that are under continuous development and not mature. Indeed, multilevel converters using more switching components can be both cheaper and more reliable than standard two-level solution with rare and more expensive

components. In addition, multilevel solution requires smaller filters to satisfy power quality requirements, which can be significant in high-power ranges. Today, multilevel converters are a good solution for power applications because they can achieve high power using mature medium-power semiconductor technology covering power range from 1 MW to 30 MW.

The maximum power limit of standard three-phase converters is bound to the maximum voltage and current limits of a switching component. Furthermore, higher the power of a switch, lower is its switching frequency. Connecting several switches in series or parallel was one of the initial solutions to overcome these limitations but the difficulty in achieving perfect synchronization of commutations creates problems in the series connection of two or more semiconductor devices. In fact, if one component switches on faster than the others, it will blow up because it will be subjected to the entire voltage drop designed for the series. However, a parallel connection is slightly less complicated due to the positive resistance coefficient property of MOSFETs and IGBTs with the increment of junction temperature. When a component switches on faster than the others do, it will conduct a current greater than the rated one which increases its junction temperature and resistance, therefore limiting the current to some extent. The problems arising from a delay among gate signals or from differences among real turn on time of the components are thus overcome due to this effect. Nevertheless, parallel connection of the switches has its limits. It requires careful and precise design of the system to achieve an almost perfect symmetry of the components, a task more difficult to maintain as their numbers rise.
Moreover, multilevel converters present several other advantages:
• Generation of better output waveforms with a lower dv/dt than standard converters (power quality).
• Growth in the power quality due to the great number of levels of the output voltage by which the AC side filters can be reduced, decreasing its costs and losses (low switching losses).
• Can operate with a lower switching frequency than two-level converters, so the electromagnetic emissions they generate are weaker, allowing it to be less severe to comply with the standards (EMC).
• Can be directly connected to high voltage sources without using transformers; this means a reduction of implementation and costs.

The main disadvantages of this technique are:
• Larger number of semiconductor switches leads to increased complexity compared to the two-level solution.
• Capacitor banks or insulated sources are required to create the DC voltage steps.

Multilevel converters are a viable solution to increase the power with a relatively low stress on the components and with simple control systems.
The most common multilevel converter topologies are [4]:
• Diode clamped (neutral-point clamped),
• Flying capacitor (capacitor-clamped),
• Cascaded topology.

MODELLING OF WIND TURBINE

The static characteristics of the turbine (output as a function of wind speed) can be described by the relationship between the total power and mechanical energy of the wind:

$$P_{wind} = \frac{1}{2}\rho\pi R_{turbine}^2 v_{wind}^3 \qquad (1)$$

Where, ρ is the air density (1,225 kg/m3), Rturbine is the rotor radius (m), vwind is the wind speed (m/s). Extracting all the kinetic energy of the wind is impossible, so, only a fraction of the power of wind is extracted as shown in (2) as the power coefficient Cp.

$$P_m = \frac{1}{2}C_p\rho\pi R_{turbine}^2 v_{wind}^3 \qquad (2)$$

Pm is the mechanical power of the wind (Nm/s). The maximum power coefficient CpM is 0.59. This coefficient is also known as Betz limit which can be expressed in terms of reduced velocity λ and angle of light θ: Cp = Cp (λ, θ).
If W is the rotor speed, then the reduced speed λ is defined by:

$$\lambda = \frac{\Omega R_{turbine}}{v_{wind}} \qquad (3)$$

Assuming a constant wind speed vwind, the reduced speed λ varies proportionally to the speed of the rotor [10]. The maximum value of Cp is generally obtained for values of λ around 8 to 9 (when the tip of the blade moves 8 to 9 times faster than the wind). In modern wind turbines, the adjustment of the blade angles is possible through a control mechanism [11]. If Cp-λ curve is known for a specific wind with a radius of turbine rotor Rturbine, it is easy to construct the curve of Cp as a function of rotational speed Ω for a wind speed vwind. The output torque of the turbine is calculated using:

$$T_m = \frac{P_m}{\Omega} = \frac{1}{2}\frac{C_p\rho\pi R_{turbine}^2 v_{wind}^3}{\Omega} \qquad (4)$$

If the speed ratio λ is maintained at its optimal value λopt, the power coefficient is at its maximum value CpM=Cp(λopt), the maximum power of the wind turbine will be:

$$P_m^{opt} = \frac{1}{2}C_{pM}\rho\pi R_{turbine}^2 v_{wind}^3 \qquad (5)$$

On the other hand, the speed ratio assumed to be maintained at the optimum value, we obtain the optimum speed of the rotor using:

$$\lambda^{opt} = \frac{\Omega R_{turbine}}{v_{wind}} \Rightarrow \Omega^{opt} = \frac{\lambda^{opt} v_{wind}}{R_{turbine}} \qquad (6)$$

Thus, the wind turbine power characteristics are shown in figure 2.1.

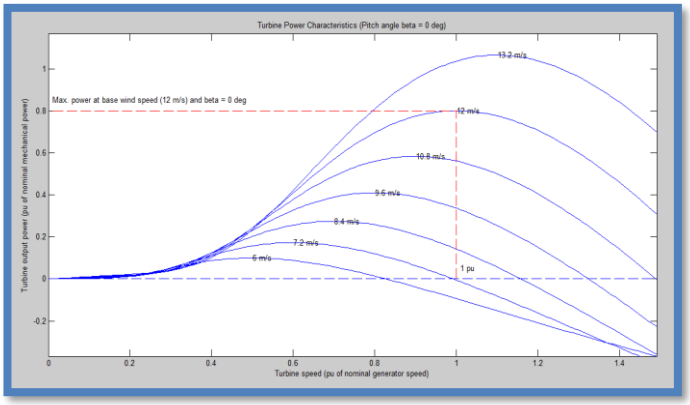

Figure 2.1: Wind Turbine Power Characteristics

In this paper, a wind turbine is simulated by using a look-up table, where inputs are wind speed and rotor speed and output is the mechanical torque.

MODELLING OF PMSM

The mathematical model for the vector control of the PMSM can be derived from its dynamic d-q model which can be obtained from well-known model of the induction machine with the equation of damper winding and field current dynamics removed. A synchronously rotating rotor reference frame is chosen so the stator winding quantities are transformed to the synchronously rotating reference frame that is revolving at rotor speed.

The model of PMSM without damper winding has been developed on rotor reference frame using the following assumptions:

Saturation is neglected.

The induced EMF is sinusoidal.

Core losses are negligible.

There are no field current dynamics.

It is also assumed that the rotor flux is constant at a given operating point and concentrated along the d axis while there is zero flux along the q axis, an assumption similarly made in the derivation of indirect vector controlled induction motor drives. Because the position of the rotor magnets independently determines the stator voltages and currents, instantaneous induced emf, and subsequently the stator currents and torque of the machine, the rotor reference frame is chosen. When rotor reference frames are considered, it means the equivalent q and d axis stator windings are transformed to the reference frames that are revolving at rotor speed. The consequence of this is that there is zero speed differentials between the rotor and stator magnetic fields and the stator q and d axis windings have a fixed phase relationship with the rotor magnet axis which is the d axis in the modelling. The stator equations of the induction machine in the rotor reference frames using flux linkages are taken into consideration to derive the model of the PMSM as shown in Fig.3.1:

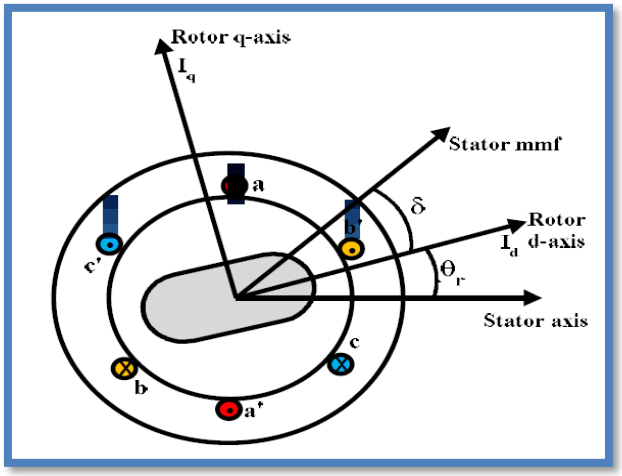

Fig.3.1: PM machine synchronously rotating d-q reference frame.

Therefore, a PM machine is described by the following set of general equations:

Voltage equations are given by:

$V_d = R_s i_d - \omega_r \lambda_q + \frac{d\lambda d}{dt}$ (1)

$V_q = R_s i_q - \omega_r \lambda_d + \frac{d\lambda d}{dt}$ (2)

Flux linkages are given by

$\lambda_q = L_q i_q$ (3)

$\lambda_d = L_d i_d + \lambda_f$ (4)

Substituting (3) & (4) into (1) & (2), we get

$V_q = R_s i_q + \omega_r (L_d i_d + \lambda_f) + \frac{d}{dt}(L_q i_q)$ (5)

$V_d = R_s i_d - \omega_r L_q i_q + \frac{d}{dt}(L_d i_d + \lambda_f)$ (6)

Arranging equations (5) and (6) in a matrix, we get

$$\begin{pmatrix} V_q \\ V_d \end{pmatrix} = \begin{pmatrix} R_s + \frac{dL_q}{dt} & \omega_r L_d \\ -\omega_r L_q & R_s + \frac{dL_d}{dt} \end{pmatrix} \begin{pmatrix} i_q \\ i_d \end{pmatrix} + \begin{pmatrix} \omega_r \lambda_f \\ \frac{d\lambda_f}{dt} \end{pmatrix}$$

the developed torque motor is being given by

$T_e = 3/2\ (P/2)\ (\lambda_d i_q - \lambda_q i_d)$ (8)

$T_e = 3/4\ P[\lambda_f i_q + (L_d - L_q)\ i_q i_d]$ (9)

The mechanical torque equation is

$T_e = T_L + B\omega_m + J\frac{d\omega m}{dt}$ (10)

Solving for rotor mechanical speed from (10), we get

$\omega_m = \int 1(T_e - T_L - B\omega_m / J)\ dt$ (11)

and rotor electrical speed is $\omega_r = \omega_m(P/2)$. (12)

MULTILEVEL INVERTER TOPOLOGY

Neutral Point-Clamped Inverter:

A three-level, diode-clamped inverter is shown in Fig. 4.1(a). The dc-bus voltage is split into three levels in this circuit by two series-connected bulk capacitors, C1 and C2. The middle point of the two capacitors n can be defined as the neutral point. The output voltage van has three states: Vdc/2, 0, and -Vdc/2. For voltage level Vdc/2, switches S1 and S2 need to be turned on; for -Vdc/2, switches S1' and S2' need to be turned on; and for the 0 level, S2 and S1' need to be turned on.

The key components that distinguish this circuit from a conventional two-level inverter are D1 and D1'. These two diodes clamp the switch voltage to half the level of the dc-bus voltage. When both S1 and S2 turn on, the voltage across a and 0 is Vdc i.e., va0 =Vdc. In this case, D1' balances out the voltage sharing between S1' and S2' with S1' blocking the voltage across C1 and S2' blocking the voltage across C2. Notice that output voltage van is ac, and va0 is dc. The difference between van and va0 is the voltage across C2, which is Vdc /2. If the output is removed between a and 0, then the circuit becomes a dc/dc converter, which has three output voltage levels: Vdc , Vdc/2, and 0.

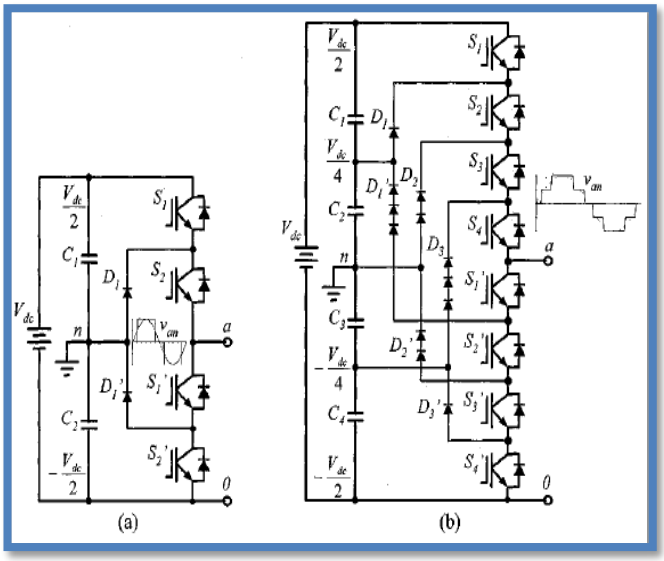

Fig. 4.1. Diode-clamped multilevel inverter circuit topologies. (a) Three-level. (b) Five-level.

Considering that m is the number of steps of the phase voltage with respect to the negative terminal of the inverter, then the number of steps in the voltage between two phases of the load k is

k = 2m+1 (1) and the number of steps p in the phase voltage of a three-phase load in wye connection is

p = 2k – 1. (2)

The term multilevel was coined by Nabae et al who introduced the three-level inverter. [3]. By increasing the number of levels in the inverter, the output voltages, with more steps, generate a staircase waveform which has a reduced harmonic distortion. However, a high number of levels increases the control complexity and introduces voltage imbalance issues.

Fig. 4.1(b) shows a five-level diode-clamped converter in which the dc bus consists of four capacitors, C1, C2, C3, and C4. For dc-bus voltage Vdc, the voltage across each capacitor is Vdc/4, and each device voltage stress will be limited to one capacitor voltage level Vdc/4 through clamping diodes.

To explain the synthesis of the staircase voltage, the neutral point n is considered as the output phase voltage reference point. There are five switch combinations to synthesize five level voltages across a and n.

1) For voltage level Van = Vdc/2, all upper switches S1– S4 are on.

2) For voltage level Van = Vdc/4, three upper switches S2– S4 and one lower switch S1'are on.

3) For voltage level Van = 0, two upper switches S3 and S4 and two lower switches S1' and S2'are on.

4) For voltage level Van = –Vdc/4, one upper switch and three lower switches S1'– S3'are on.

5) For voltage level Van = –Vdc/2, all lower switches S1'– S4'are on.

Four complementary switch pairs are used in each phase. The switch pairs are termed complementary as turning on one of the switches will exclude the other from being turned on. In this example, the four complementary pairs are (S1, S1'), (S2, S2'), (S3, S3'), and (S4, S4').

TABLE- I: Switching States of the Five-Level Inverter

Output	Switch States							
v_{a0}	S_1	S_2	S_3	S_4	S_1'	S_2'	S_3'	S_4'
$V_3=V_{dc}$	1	1	1	1	0	0	0	0
$V_4=3V_{dc}/4$	0	1	1	1	1	0	0	0
$V_3=V_{dc}/2$	0	0	1	1	1	1	0	0
$V_2=V_{dc}/4$	0	0	0	1	1	1	1	0
$V_1=0$	0	0	0	0	1	1	1	1

Although each active switching device is only required to block a voltage level of Vdc /(m-1), the clamping diodes must have different voltage ratings for reverse voltage blocking. Using D1'of Fig. 2(b) as an example, when lower devices S2' ~ S4' are turned on, D1' needs to block three capacitor voltages, or 3Vdc/4. Similarly, D2 and D2' need to block 2Vdc/4, and D3 needs to block 3Vdc/4. Assuming that each blocking diode voltage rating is the same as the active device voltage rating, the number of diodes required for each phase will be (m-1) (m-2). This number represents a quadratic increase in m. When m is sufficiently high, the number of diodes required will make the system impractical to implement. Also, the diode reverse recovery of these clamping diodes becomes a major design challenge in high-voltage high-power applications if the inverter runs under PWM.

SIMULATION & RESULTS

The simulation system of an 11-level NPC multi-level inverter with renewable energy resources in to AC grid is validated by simulation of the circuit in MATLAB/SIMULINK environment.

The entire wind energy conversion system is as shown in figure. The wind energy is captured by the blades of the turbine and the energy is transferred to the turbine rotor which is connected to a common shaft connecting the PMSG. The mechanical energy is converted by the PMSG to three phase ac voltage which fluctuates in relation to the wind speed. The three phase ac voltage is then converted into dc using a three-phase rectifier. Output dc voltage is fed to a boost converter which boosts the input signal voltage and feeds an amplified dc voltage to the MLI. The NPC topology of the MLI blocks

the dc component from entering the grid and provides feasible application of control technique for the switches.

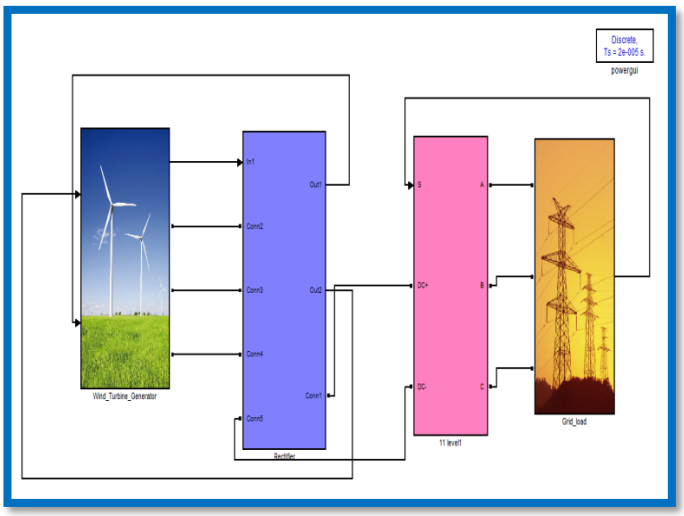

Figure 5.1: Schematic Model of AC grid connected renewable energy resources with NPC Multi Inverter

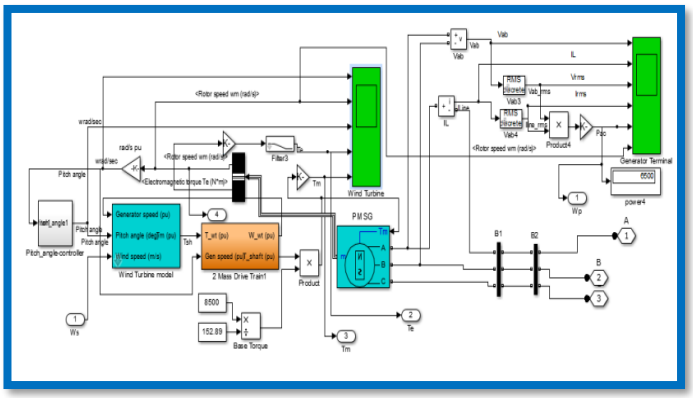

Figure 5.2: Wind power generation by using PMSG

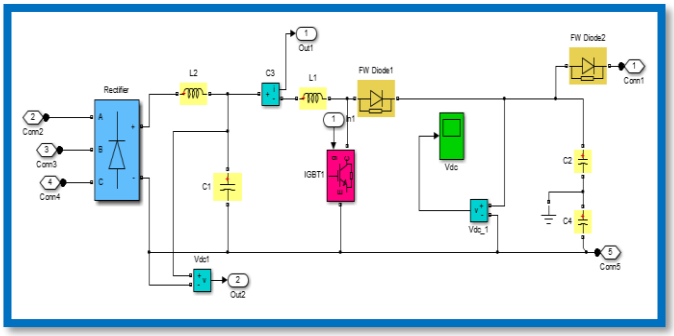

Figure 5.3: Simulink of Rectifier

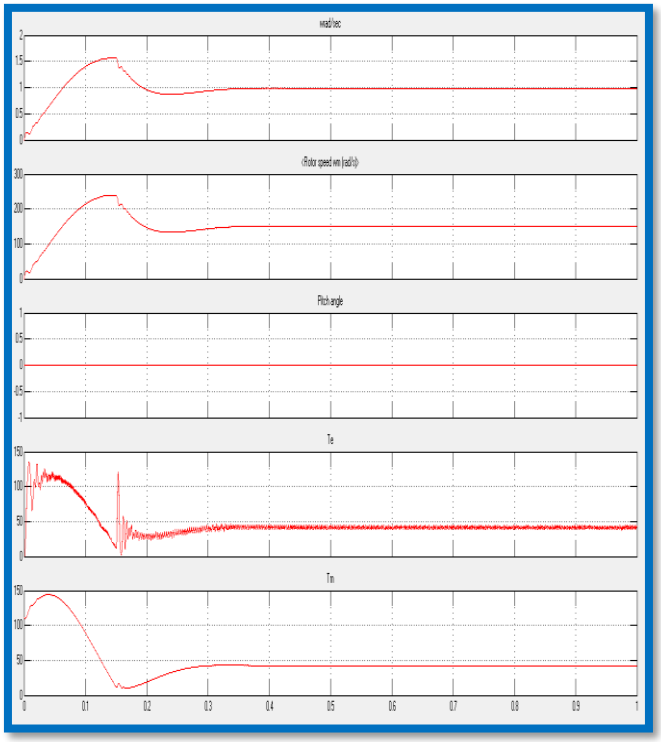

Figure 5.4: Waveform of Wind Turbine (a) wind Speed (b) Rotor speed (c) Pitch angle (d) Electromagnetic Torque (e) Mechanical Torque.

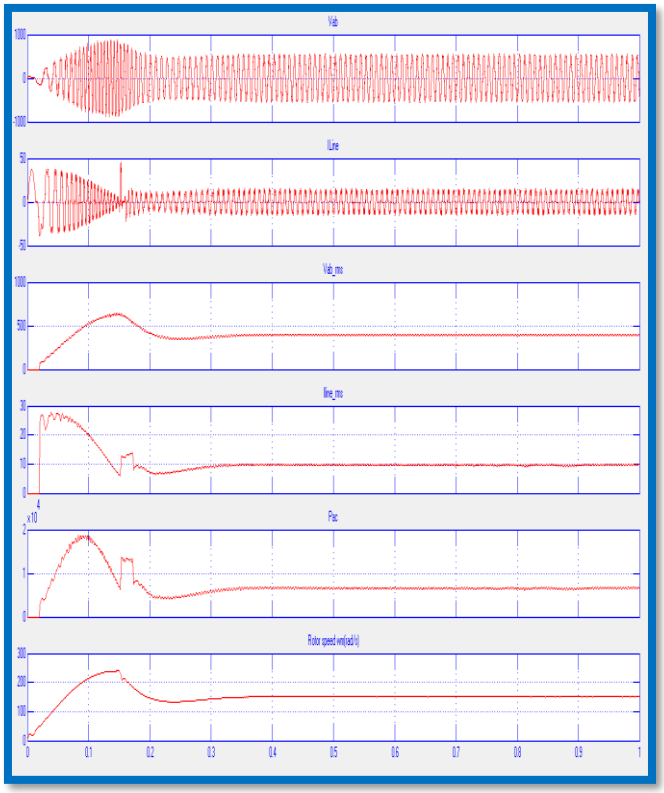

Figure 5.5: Waveform of Generator Terminal (a) Voltage at Stator terminal of ab (b) Current of Line (c) RMS Voltage at Stator terminal of ab (d) RMS current of Line (e) Generated Power (f) Rotor Speed.

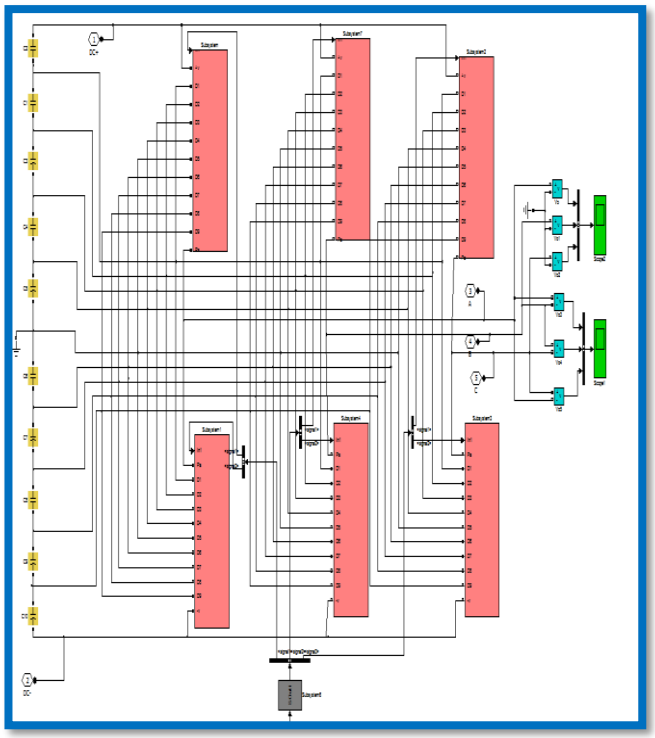

Figure 5.6: Simulink model of 11 level NPC multi inverter

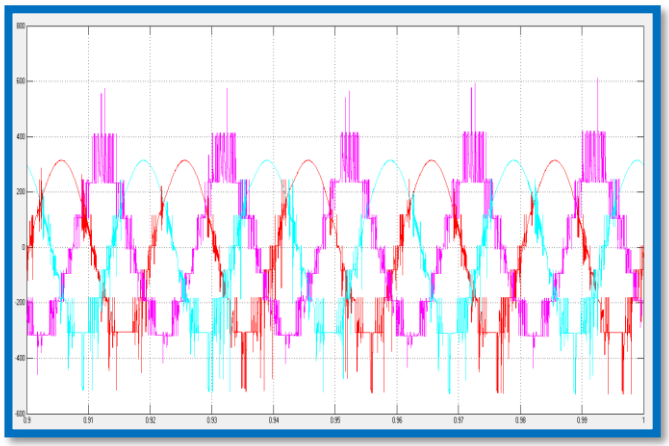

Figure 5.7: Output waveform of Upper half 11 level NPC multi inverter

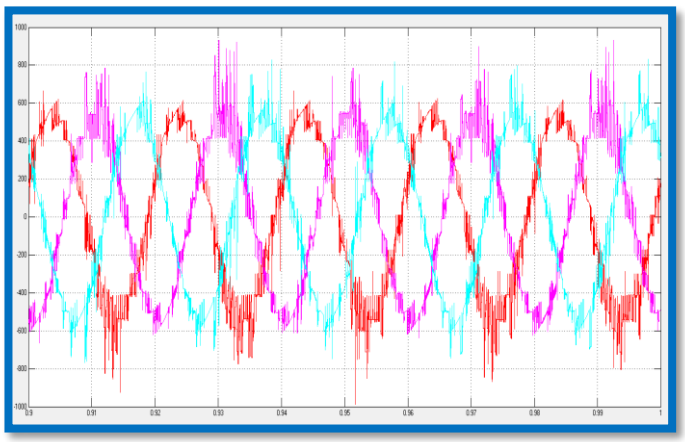

Figure 5.8: Output waveform of Lower half 11 level NPC multi inverter

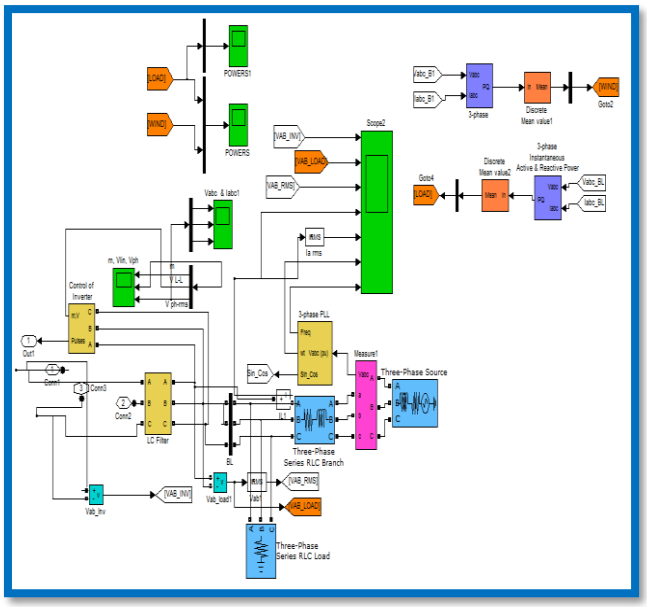

Figure 5.9: Simulink Model of AC Grid Connected Load

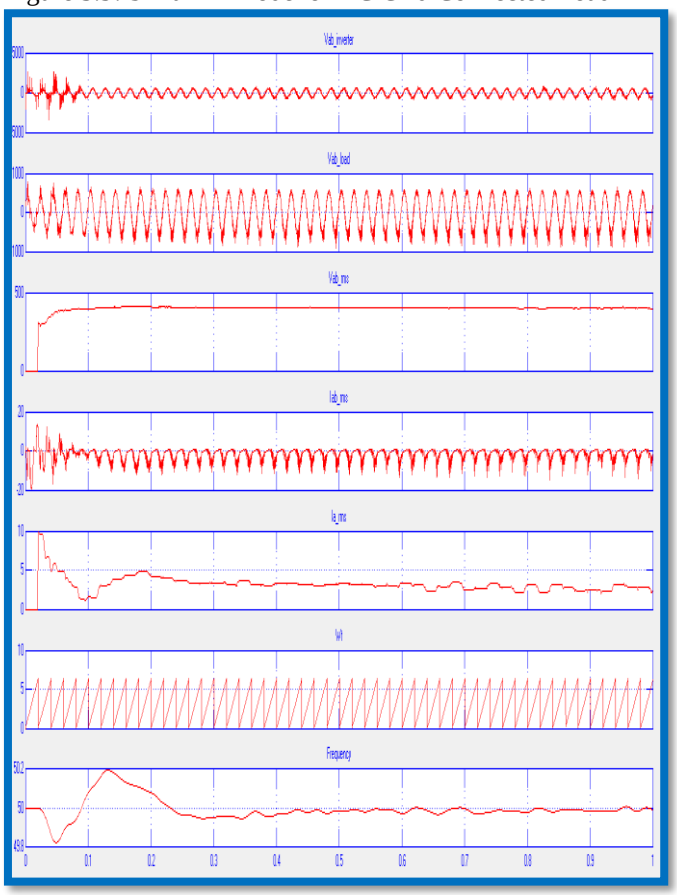

Figure 5.10: Waveform of AC Grid Connected Load (a) Voltage at Inverter (b) Voltage at Load (c) RMS Voltage at Inverter (d) RMS current of Load at terminal ab (e)) RMS current of Load at terminal ab (f) Rotor Speed (g) Frequency .

CONCLUSION

In this paper, the performance of an eleven-level NPC inverter to integrate renewable energy resource in to AC grid was presented. Using the Eleven-level NPC Converter, the output harmonics of the whole system is effectively reduced while improving power capacity of whole equipment, and reducing

the voltage stress of the switch and the equivalent switching frequency. With varying wind speeds, the voltage and current also vary which in turn affects the grid power. As wind speed decreases, the active and reactive power also decreases. The pitch angle controller is used to control the blade angle at θ = 0. Simulations show that generator side can realize the maximum wind power tracking, and makes the generator operate stably and efficiently by using double closed loop control based on maximum ratio of torque to current. The grid side converter adopts the vector control of grid voltage orientation, realizing the decoupling control of the active and reactive power. Alongside feeding the grid with high quality electrical energy, it also improves the utilization of the whole system. Here an LC filter is used to remove the harmonics available in the system and MPPT is used to track the maximum power. In conclusion, with the information stated above, it is clear that as the inverter levels increase, line and phase voltage waveform also increases and the induced harmonics decrease. Simulation results clarified the ability of the control scheme in compensation of load active and reactive power. We can observe that using an eleven-level NPC inverter, the THD is less compared to using a nine-level NPC inverter as an interfacing circuit to integrate renewable energy into an AC grid. From the FFT analysis of a nine-level NPC inverter and an eleven-level NPC inverter, the THD of the nine-level is 12.87% while the THD of the eleven-level NPC inverter is 4.38%. This goes on to prove that as the level of the inverter increases, the THD decreases. The proposed control scheme is capable to be used in all types of converter topologies and can be used as a multi objective strategy for integration of renewable energy resources into AC grids.

REFERENCE

A. Nasiri, O. Abdel-Baqi, and B. Novakovic, "A Hybrid System of Li-Ion Capacitors and Flow Battery for Dynamic Wind Energy Support," IEEE 2013.

A. Nabae, I. Takahashi, and H. Akagi, "A new neutral-point clamped PWM inverter,"IEEE Trans. Sep. 1981.

AkieUehara, AlokPratap, Tomonori Goya. A Coordinated Control Method to Smooth Wind Power Fluctuations of a PMSG-Based WECS[J].IEEE Transactions on Energy Conversion, Vol.26,No.2, 2011

B. Boukhezzar and H. Siguerdidjane, "Nonlinear control of a variable-speed wind turbine using a two-mass model," IEEE Trans. 2011.

B. M. Delghavi, A. Yazdani, "An Adaptive Feedforward Compensation for Stability Enhancement in Droop-Controlled Inverter-Based Microgrids," IEEE Transactions on Power Delivery 2011.

Edris Pouresmaeil, Daniel Montesinos-Miracle, and Oriol Gomis Bellmunt "Control Schem of Three-Level NPC Inverter for Integration of Renewable Energy Resources into AC Grid"", IEEE 2012.

F. Carnielutti, H. Pinheiro, and C. Rech, "Generalized carrier-based modulation strategy for cascaded multilevel converters operating under fault conditions," IEEE Trans. Ind. Electron Feb. 2012.

G. Delille, B. Francois, and G. Malarange, "Dynamic Frequency Control Support by Energy Storage to Reduce the Impact of Wind and Solar Generation on Isolated Power System's Inertia," IEEE 2012.

G. Mandic and A. Nasiri "Modeling and Simulation of a Wind Turbine System with Ultracapacitors for Short-Term Power Smoothing," in Proc. IEEE International Symposium on Industrial Electronics, July 2010 Italy.

L. Serpa, S. Ponnaluri, P. Barbosa, J. Kolar, " A modified direct power control strategy allowing the connection of three-phase inverters to the grid though LCL filter," IEEE 2007, Page(s) 1388-1400.

Mukhtiar Singh, Vinod Khadkikar, Ambrish Chandra, and Rajiv K. Varma, "Grid Interconnection of Renewable Sources at the Distribution Level With Power Quality Improvement Features", IEEE 2011.

N. R. Ullah, T. Thiringer, and D. Karlsson, "Voltage and Transient Stability Support by Wind Farms Complying With the E.ON Netz Grid Code," IEEE Transactions on Power Systems, vol. 22, no. 4, pp. 1647-1656, 2007.

S. Alepuz, S. Busquets-Monge, J. Bordonau, J. Gago, D. Gonzalez, and J. Balcells,"Interfacing renewable energy source to the utility grid using a three-level inverter,"IEEE Trans. Ind Oct. 2006.